# Exploring the scattering characteristics of twisted vortex electromagnetic light waves with a PEMC sphere in isotropic plasma

FAROQ RAZZAZ[1,*], MUHAMMAD ARFAN[2]
[1]*Electrical Engineering Department, College of Engineering, Prince Sattam Bin Abdulaziz University, Al-Kharj 16278, Saudi Arabia*
[2]*Department of Physics, University of Agriculture, Faisalabad 38000, Pakistan*

Vortex beams (VBs) carrying orbital angular momentum (OAM) have recently fascinated a lot of consideration. The inclusion of OAM in vortex beams makes them exceptionally versatile for several applications. So, inspired by the exciting uses of vortex electromagnetic waves (VEMWs), this work examines how twisted light waves like VEMWs interact with a metamaterial perfect electromagnetic conductor (PEMC) sphere in an isotropic plasma medium. Influences of configuration parameters of an isotropic plasma, i.e., plasma density and effective collision frequency, on the scattered field distributions of VEMWs are examined numerically. The study's results might be useful for understanding how different metamaterials interact with VEMWs when subjected to isotropic plasma.

(Received May 7, 2025; accepted December 2, 2025)

*Keywords:* Vortex electromagnetic wave, Orbital angular momentum, PEMC sphere, Metamaterials, Isotropic plasma, Scattered field distributions

## 1. Introduction

Since their inception [1], VBs have been widely researched, leading to important developments like using OAM for particles manipulation and creating devices that shape beams. VBs are mesmerizing because of a property called phase singularity. This singularity may be measured by an integer called topological charge or beam order, which indicates the number of times the phase profile winds around the optical beam center within the intermission period $[0, 2\pi]$[2]. VBs have sparked attention in the field of twisted light owing to their distinct phase and polarization features, making them suitable for various potential applications [3, 4]. Combining VBs with isotropic materials allows for new ways to change and control electromagnetic fields in nonlinear optics [5]. These applications require a sophisticated modeling that considers isotropic materials and VBs.

The phase profile and intensity distribution of VBs result in unique scattering characteristics that markedly differ from classical Lorenz-Mie scattering, which addresses plane wave interactions with homogeneous spherical particles [6]. Consequently, there has been significant interest in investigating the scattering features of different families of vortex beams from particles. Consequently, there has been a growing attention in multiple disciplines regarding the investigation and utilization of the properties of VBs, including applications in light propagation, scattering, sensing, and communications [7-9].

Metamaterials have garnered significant interest within the research community owing to their unique properties for electromagnetic applications [10]. The field of optics and photonics has strong recommendations for these man-made materials. Consequently, various practical initiatives have been implemented to create innovative devices utilizing metamaterials for diverse applications [11]. Metamaterials consist of multiple sub-wavelength compositional components. They execute numerous critical functions, including wave amplitude, polarization, and spatial phase profile. Characteristics like compact size, affordability, effective performance, and seamless environmental integration contribute to their preference [12].

The PEMC is a notable example of metamaterials [13, 14]. The phrase “(PEMC) materials” encompasses both perfect electric conductor (PEC) and perfect magnetic conductor (PMC) materials [15]. No electromagnetic waves can be contained within a PEMC medium. The interaction of electromagnetic waves with the PEMC medium is intriguing and presents complex applications in resonators and waveguides [16]. The PEMC can change the direction of the incoming light's polarization by creating scattered electromagnetic waves that are both cross-polarized and co-polarized as they move through the propagation medium [17].

The investigation of plasma-based composite metamaterials has attracted significant attention within the research community [18]. Plasma, newly identified as a metamaterial, has demonstrated potential applications in communication systems, defense technologies, and plasma

photonic crystals [19]. To improve the electromagnetic scattering properties of a wide range of materials, several researchers have turned to plasmas as covering objects [20, 21].

A number of critical parameters, such as the frequency of incident light waves, collisional frequency, number density of electrons, and plasma frequency, determine the optical characteristics of electromagnetic waves in plasma [22]. Plasma exhibits unique characteristics compared to traditional dielectrics. A significant benefit of plasma in nanophotonic devices is its capacity to diminish absorption losses. These losses can be reduce by adding plasma, a low-loss medium that efficiently reduces absorption and increases light transmission [23]. Additionally, some researchers have investigated an in-depth examination of plasma-coated objects [23, 24].

Many researchers also studied and analyzed the interaction of the PEMC scatterer with an anisotropic plasma medium. Scattering by an anisotropic plasma-coated PEMC cylinder has been done [25]. Transverse electric (TE) polarized wave interaction with a PEMC slit surrounded by an anisotropic plasma medium has been explored [26]. The influence of plasma frequency and number density for RCS of a metamaterial PEMC sphere subjected to a layer of anisotropic plasma was studied [27]. Electromagnetic scattering from an anisotropic plasma-covered PEMC cylinder suppressed under a rough surface has been investigated [28]. The scattering characteristics of a plane wave by a PEMC cylinder in an anisotropic plasma medium have been considered [29].

The study of OAM of light beams and the conversion of the Laguerre-Gaussian (LG) beam was analyzed [1]. The scattering of light with OAM from gold nanoparticles has been investigated [30]. The backscattering characteristics of the VEMW across different OAM modes have been examined [31]. Scattering characteristics of VEMW in relation to a wedge were discussed [32]. The scattering analysis of VEMW across various OAM modes using a coated sphere has been debated [33]. The distributions of the scattered fields from a metallic sphere vary with changes in the OAM mode number, as analyzed in reference [34]. Structured light wave scattering by a PEMC sphere has been numerically analyzed [35, 36].

But as far as we are aware, no one has yet documented the detailed reports regarding the attributes of VEMW scattering in the PEMC sphere in an isotropic plasma. It is possible that the VEMW will display several intriguing characteristics when they scatter via metamaterial PEMC media in the presence of an isotropic plasma.

This article is structured as follows: In section 2, an analytical model of the work is introduced. Section 3 computes and discusses the numerical results. Section 4 discusses the final thoughts and findings of this research.

## 2. Theoretical formulations

In Fig. 1, the interaction model is drawn. Consider the beam field of a polarized LG VEMW that illuminates the PEMC sphere with radius $a$ in an isotropic plasma medium. Wave propagation is along the $z$-axis, and its polarization is about the $x$-axis.

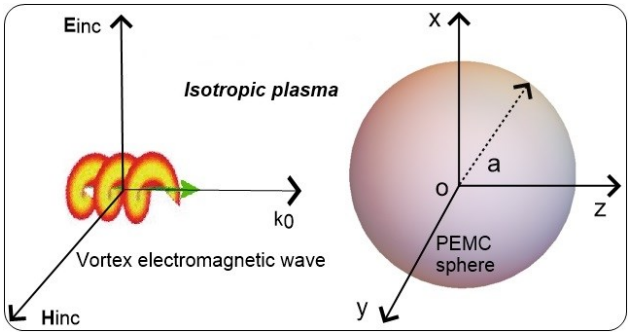


*Fig. 1. Interaction model of the problem (colour online)*

An expression for the incident electric field of the LG VEMW is as follows:

$$\boldsymbol{E}^{inc}(r_t,\varphi,z) = E_0\left(\frac{r_t\sqrt{2}}{w_0}\right)^{l}\exp\left(\frac{-r_t^2}{w_0^2}\right)\exp i(kz - \\ -l\varphi)\left(sin\theta cos\varphi\hat{\boldsymbol{r}} + cos\theta cos\varphi\hat{\boldsymbol{\theta}} - sin\varphi\hat{\boldsymbol{\varphi}}\right) \quad (1)$$

where $r_t = r\,cos\theta$ $(0 \le \theta \le \pi)$ while, $w_0$ represents beam waist radius. The incidence electromagnetic fields for the LG VEMW are expressed using spherical vector wave functions (SVWFs).

$$\boldsymbol{E}^{inc} = \sum_{m=l\pm1}^{\infty}\sum_{n=m}^{\infty}\left(B_{emn}^{inc}\boldsymbol{M}_{emn}^{(1)} + B_{omn}^{inc}\boldsymbol{M}_{omn}^{(1)} + \\ +A_{emn}^{inc}\boldsymbol{N}_{emn}^{(1)} + A_{omn}^{inc}\boldsymbol{N}_{omn}^{(1)}\right) \quad (2)$$

$$\boldsymbol{H}^{inc} = -\left(\frac{1}{\eta_0}\right)\sum_{m=l\pm1}^{\infty}\sum_{n=m}^{\infty}\left(B_{emn}^{inc}\boldsymbol{N}_{emn}^{(1)} + B_{omn}^{inc}\boldsymbol{N}_{omn}^{(1)} + \\ +A_{emn}^{inc}\boldsymbol{M}_{emn}^{(1)} + A_{omn}^{inc}\boldsymbol{M}_{omn}^{(1)}\right) \quad (3)$$

The wavenumber in an isotropic plasma region can be denoted as $k = k_0\sqrt{\varepsilon_p}$, with $k_0 = \frac{2\pi}{\lambda}$ be the free space wave number. $\varepsilon_p$ denotes relative permittivity regarding an isotropic plasma such as $\varepsilon_p = 1 - \frac{i\omega_0^2}{\omega(v+i\omega)}$ with $\omega_0$ represents plasma frequency $\omega_0 = (\frac{ne^2}{m\varepsilon_0})^{1/2}$. The term $v$ indicates effective collision frequency.

$B_{emn}^{inc}$, $B_{omn}^{inc}$, $A_{emn}^{inc}$, and $A_{omn}^{inc}$ represent the unknown scattering coefficients associated with the incident VEMW. Utilizing the orthogonality characteristics of SVWFs, the undetermined coefficients can be found by employing the inner product of incident electric field Eq. (2) just like that

$$B_{emn}^{inc} = \frac{\int_0^{2\pi}\int_0^{\pi}\boldsymbol{E}^{inc}.\boldsymbol{M}_{emn}^{(1)}\,sin\theta\,d\theta d\varphi}{\int_0^{2\pi}\int_0^{\pi}\left|\boldsymbol{M}_{emn}^{(1)}\right|^2 sin\theta\,d\theta d\varphi} \quad (4)$$

$$B_{omn}^{inc} = \frac{\int_0^{2\pi}\int_0^{\pi}\boldsymbol{E}^{inc}.\boldsymbol{M}_{omn}^{(1)}\,sin\theta\,d\theta d\varphi}{\int_0^{2\pi}\int_0^{\pi}\left|\boldsymbol{M}_{omn}^{(1)}\right|^2 sin\theta\,d\theta d\varphi} \quad (5)$$

$$A_{emn}^{inc} = \frac{\int_0^{2\pi}\int_0^{\pi} \boldsymbol{E}^{inc}.\boldsymbol{N}_{emn}^{(1)} \sin\theta \, d\theta d\varphi}{\int_0^{2\pi}\int_0^{\pi} \left|\boldsymbol{N}_{emn}^{(1)}\right|^2 \sin\theta \, d\theta d\varphi} \quad (6)$$

$$A_{omn}^{inc} = \frac{\int_0^{2\pi}\int_0^{\pi} \boldsymbol{E}^{inc}.\boldsymbol{N}_{omn}^{(1)} \sin\theta \, d\theta d\varphi}{\int_0^{2\pi}\int_0^{\pi} \left|\boldsymbol{N}_{omn}^{(1)}\right|^2 \sin\theta \, d\theta d\varphi} \quad (7)$$

The corresponding electromagnetic fields for the scattered LG VEMW are denoted as [35]

$$\boldsymbol{E}^{sca} = \sum_{m=l\pm1}^{\infty}\sum_{n=m}^{\infty}\left(b_{emn}^{sca}\boldsymbol{M}_{emn}^{(3)} + b_{omn}^{sca}\boldsymbol{M}_{omn}^{(3)} + a_{emn}^{sca}\boldsymbol{N}_{emn}^{(3)} + a_{omn}^{sca}\boldsymbol{N}_{omn}^{(3)}\right) \quad (8)$$

$$\boldsymbol{H}^{sca} = -\left(\frac{1}{\eta_0}\right)\sum_{m=l\pm1}^{\infty}\sum_{n=m}^{\infty}\left(b_{emn}^{sca}\boldsymbol{N}_{emn}^{(3)} + b_{omn}^{sca}\boldsymbol{N}_{omn}^{(3)} + a_{emn}^{sca}\boldsymbol{M}_{emn}^{(3)} + a_{omn}^{sca}M_{omn}^{(3)}\right). \quad (9)$$

The expressions for scattered electromagnetic fields in Eqs. (8) and (9) are achieved by employing the standard theory of electromagnetic scattering [30, 35, 37, 38]. The incident LG vortex electromagnetic wave is initially written in the context of SVWFs; afterwards, the BCs on the spherical surface of the PEMC sphere are implemented to find the unknown coefficients for the scattered field. The substitution of these expansion coefficients into the spherical-wave expression yields the closed form of scattered electromagnetic fields. Furthermore, applying the PEMC BCs at $r = a$, besides matching the components of electromagnetic fields, it forms a system of linear equations that are solved for coefficients of scattered fields.

Taking into account the factor $m$, the selection rule is established as

$$m = \begin{cases} 1 & l = 0 \ (plane\ wave) \\ l \pm 1 & l \neq 0 \ (VEMW) \end{cases} \quad (10)$$

Following are the tangential and radial boundary conditions (BCs) that can be used to obtain these unknown scattering coefficients from the boundary of the PEMC sphere [39].

$$\boldsymbol{H}^{inc}\big|_{t(r=a)} + M\boldsymbol{E}^{inc}\big|_{t(r=a)} + \boldsymbol{H}^{sca}|_{t(r=a)} + M\boldsymbol{E}^{sca}|_{t(r=a)} = 0 \quad (11)$$

$$\epsilon_0\boldsymbol{E}^{inc}\big|_{r(r=a)} + \epsilon_0\boldsymbol{E}^{sca}|_{r(r=a)} - M\mu_0\boldsymbol{H}^{inc}\big|_{r(r=a)} \mp M\mu_0\boldsymbol{H}^{sca}|_{r(r=a)} = 0 \quad (12)$$

Tangential signifies the electromagnetic fields that act about the surface of the metamaterial PEMC sphere; it manages coupling of the surface modes, while the radial part indicates the electromagnetic fields that point into or out of the PEMC surface; it modifies how strongly the OAM wave interacts with the surface of the PEMC sphere. The PEMC metamaterial enforces a mixture of both electric and magnetic fields, i.e., electromagnetic fields, generally known as field action at the PEMC surface.

Extensive calculations yield the following unknown scattering coefficients for the VEMW.

$$a_{omn}^{sca} = -A_{omn}^{inc}\frac{(h_n(\rho)[\rho h_n(\rho)]' + M^2\eta_0^2 h_n(\rho)[\rho j_n(\rho)]')}{h_n(\rho)[\rho h_n(\rho)]'(1+M^2\eta_0^2)} - iM\eta_0 B_{omn}^{inc}\frac{(j_n(\rho)[\rho h_n(\rho)]' - h_n(\rho)[\rho j_n(\rho)]')}{h_n(\rho)[\rho h_n(\rho)]'(1+M^2\eta_0^2)} \quad (13)$$

$$b_{omn}^{sca} = -B_{omn}^{inc}\frac{(h_n(\rho)[\rho j_n(\rho)]' + M^2\eta_0^2 j_n(\rho)[\rho h_n(\rho)]')}{h_n(\rho)[\rho h_n(\rho)]'(1+M^2\eta_0^2)} - iM\eta_0 A_{omn}^{inc}\frac{(h_n(\rho)[\rho j_n(\rho)]' - h_n(\rho)[\rho h_n(\rho)]')}{h_n(\rho)[\rho h_n(\rho)]'(1+M^2\eta_0^2)} \quad (14)$$

$$a_{emn}^{sca} = -A_{emn}^{inc}\frac{(j_n(\rho)[\rho h_n(\rho)]' + M^2\eta_0^2 h_n(\rho)[\rho j_n(\rho)]')}{h_n(\rho)[\rho h_n(\rho)]'(1+M^2\eta_0^2)} - iM\eta_0 B_{emn}^{inc}\frac{(j_n(\rho)[\rho h_n(\rho)]' - h_n(\rho)[\rho j_n(\rho)]')}{h_n(\rho)[\rho h_n(\rho)]'(1+M^2\eta_0^2)} \quad (15)$$

$$b_{emn}^{sca} = -B_{emn}^{inc}\frac{(h_n(\rho)[\rho j_n(\rho)]' + M^2\eta_0^2 j_n(\rho)[\rho h_n(\rho)]')}{h_n(\rho)[\rho h_n(\rho)]'(1+M^2\eta_0^2)} - iM\eta_0 A_{emn}^{inc}\frac{(h_n(\rho)[\rho j_n(\rho)]' - j_n(\rho)[\rho h_n(\rho)]')}{h_n(\rho)[\rho h_n(\rho)]'(1+M^2\eta_0^2)} \quad (16)$$

where $\rho = ka$ specifies the radius of the PEMC sphere. $M$ characterizes the PEMC interface, referred to as the electromagnetic admittance. $M = 0$ corresponds to the PMC scenario, while $M$ approaching $\pm\infty$ results in the PEC condition. For $(0 \leq M \leq \infty)$, it acts as a PEMC. Theoretically, it is demonstrated that PEMC metamaterial functions as an ideal reflector for all types of electromagnetic waves, so there is no internal electromagnetic field for metamaterial PEMC structures.

For numerical results, the radar cross section (RCS) of PEMC sphere in an isotropic plasma medium can be expressed as

$$\sigma(180^0) = \left(\frac{2}{\rho}\right)^2\left[\left|\sum_{n=1}^{\infty}(-1)^n\left(n+\frac{1}{2}\right)(a_{omn}^s - a_{emn}^s)\right|^2 + \left|\sum_{n=1}^{\infty}(-1)^n\left(n+\frac{1}{2}\right)(b_{omn}^s + b_{emn}^s)\right|^2\right] \quad (17)$$

$$\sigma(0^0) = \left(\frac{2}{\rho}\right)^2\left[\left|\sum_{n=1}^{\infty}(-1)^n\left(n+\frac{1}{2}\right)(a_{omn}^s + a_{emn}^s)\right|^2 + \left|\sum_{n=1}^{\infty}(-1)^n\left(n+\frac{1}{2}\right)(b_{omn}^s - b_{emn}^s)\right|^2\right] \quad (18)$$

## 3. Numerical results and discussion

In this section, the derived formulas for electromagnetic scattering of LG VEMW from the PEMC sphere in an isotropic plasma are solved numerically. The acquired findings are shown graphically, providing the physical insights into the problem. To verify the correctness of our work, we compared the results when the plasma medium is replaced with free space dielectric. It has been noted that our findings align with the existing literature [35]. It demonstrates a favourable comparison between our results and the published literature.

The pertinent parameters of the LG VEMW and the PEMC scatterer are established as follows unless mentioned otherwise: radial mode number $p = 0$, OAM mode index or topological charge $l = 1$, beam waist radius $w_0 = 0.1 * \lambda$, and $a = 0.1 * \lambda$. The dimensionless variable

alpha ($\alpha$) is employed in lieu of the PEMC characteristic admittance parameter $M\eta_0$, and it can be expressed as $\tan\alpha = M\eta_0$. Its characteristics can be understood as

$$\alpha = \begin{cases} 0^{\circ} & M\eta_0 = 0\ (PMC) \\ 90^{\circ} & M\eta_0 = \infty\ (PEC) \\ ]0^{\circ} - 90^{\circ}[ & (PEMC) \end{cases} \tag{19}$$

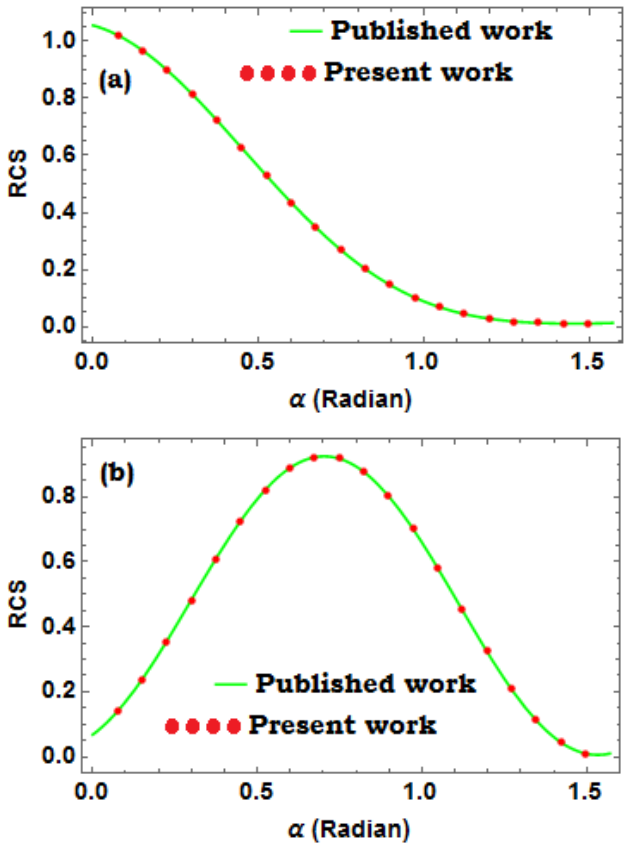


*Fig. 2. A comparison of the RCS for the LG VEMW for PEMC sphere in an isotropic plasma medium. The upper graphical result in Fig. 2(a) show the co-polarized components and the lower graphical result in Fig. 2(b) shows the cross-polarized components (colour online)*

After an effective comparison with the published literature, further results, considering the metamaterial PEMC sphere as a scatterer when subjected to isotropic plasma, are presented. Figs. 3 and 4 demonstrate how various plasma configuration characteristic parameters, such as number density ($n$) and collision frequency ($v$), influence the RCS.

To better illustrate the influence of the scattering medium on RCS more clearly, Fig. 3 shows the relationship between the RCS of LG VEMW with electron number density. From Fig. 3, it can be clearly realized that the RCS represses with the increase of electron number density.

Elevated electron number density results in pronounced dispersion, augmented attenuation of the electromagnetic wave within the isotropic plasma (attributable to the permittivity), and diminished electromagnetic field strength at the boundary of the PEMC scatterer, leading to scattering. The outcome is a diminished scattered electromagnetic field in the co-polarized and cross-polarized scattered components due to less incoming energy interaction with the metamaterial PEMC sphere.

A thick plasma functions as a shield, partially reflecting and refracting the incident LG VEMW prior to its arrival at the surface of the PEMC scatterer. Consequently, the efficiency of irradiation on the scatterer diminishes. This diminished field interaction results in a decreased RCS. Since wave impedance and the phase velocity in an isotropic plasma are subject to modification with electron number density, the scattering pattern underwent variations. The BCs at the PEMC surface are unchanged, while the characteristics of the incoming wave are modified, leading to a decrease in the intensity of both co- and cross-polarized scattered fields. In a co-polarized field, the direct reflection decreases as reduced energy impinges onto the PEMC sphere. However, for cross-polarized fields, this component frequently arises from polarization conversion at the PEMC scatterer, which is further diminished owing to reduced electromagnetic field strength at the surface of the PEMC sphere.

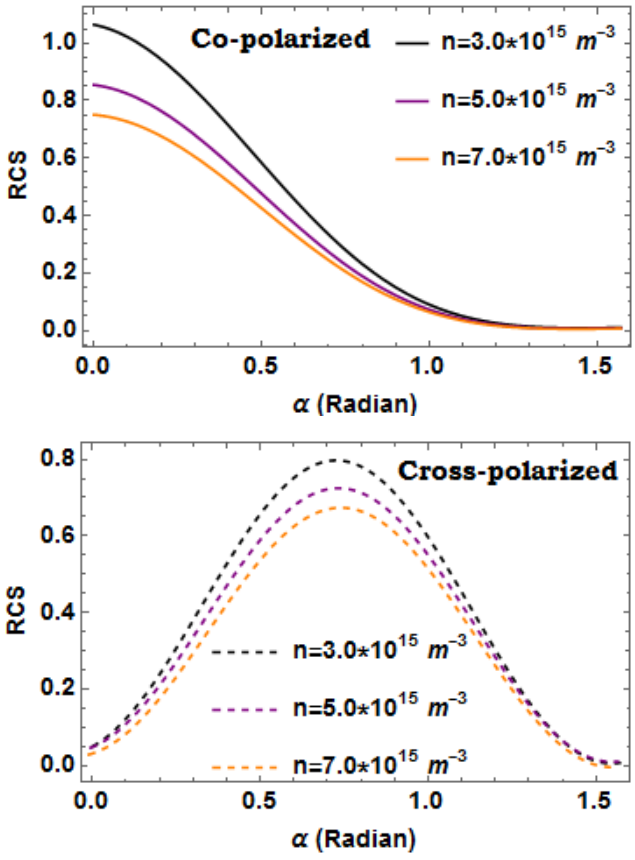


*Fig. 3. Impact of number density ($n$) on the metamaterial PEMC sphere in the presence of an isotropic plasma (colour online)*

Augmenting the electron number density results in enhancing plasma frequency and reducing relative

permittivity, resulting in LG VEMW attenuation. All these factors contribute toward diminishing contact with the PEMC sphere. This consequently decreases the RCS for both co- and cross-polarized scattered fields.

Fig. 4 illustrates the variation in RCS in relation to PEMC admittance across various collisional frequency values. Increasing the collision frequency results in increasing the scattered field for both the co-polarized and cross-polarized components. The increase in effective collision frequency correlates with an augmentation in the RCS due to the permittivity of the isotropic plasma. It comprises two parts, i.e., real and imaginary. The real part of permittivity shows its transmission ability, while the imaginary part indicates its absorption. The effective collision frequency $(v)$ has an inverse relationship with the imaginary component. Increasing $v$ results in increasing transmission while decreasing absorption.

The RCS of a PEMC sphere within an isotropic plasma medium is influenced by the interaction of VEMW with the plasma and the PEMC scatterer. The collisional frequency $(v)$ is a fundamental plasma parameter that quantifies the frequency of electron collisions with neutral atoms or ions.

In an isotropic plasma, an increase in the collision frequency $(v)$ results in amplification of the scattered field distributions for the metamaterial PEMC sphere. The permittivity becomes more complicated with a larger imaginary part, leading to greater energy loss and absorption near the PEMC sphere. This results in enhanced energy dissipation around the PEMC sphere, thereby increasing the effective scattering and, consequently, the RCS.

At low collisional frequencies, plasma exhibits characteristics that are comparable to a low-loss dielectric, particularly at frequencies exceeding the plasma frequency. However, an increase in collisional frequency diminishes this transparency, resulting in a medium that is opaquer to VEMW. A greater amount of wave energy interacts with the surface of the PEMC sphere, rather than passing through or being weakly scattered, thus increasing the electromagnetic scattering strength.

The frequency of collisions significantly modifies the wave impedance of an isotropic plasma. The difference at the plasma-PEMC boundary increases the optical features of VEMW, like reflection and scattering, which boosts both the co- and cross-polarized parts of RCS.

With an increase in collisional frequency $v$, plasma exhibits enhanced interactions with incident VEMW, resulting in increased wave scattering, absorption, and reflection. The combined effects increase the RCS of a PEMC sphere for both co-polarized and cross-polarized components.

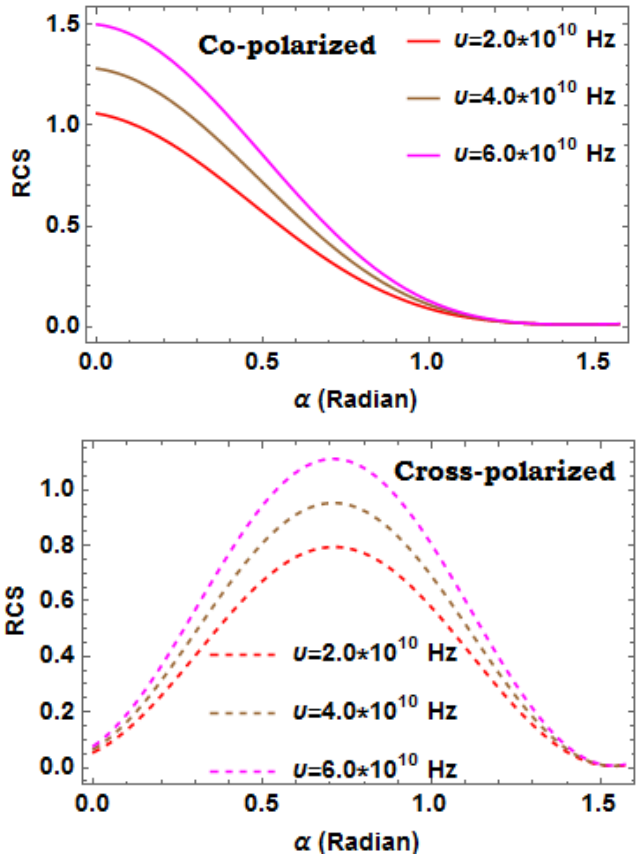


*Fig. 4. Impact of effective collision frequency $(v)$ on the metamaterial PEMC sphere in the presence of an isotropic plasma (colour online)*

In Fig. 5, density plots under electron number density $(n)$ and effective collision frequency $(v)$ with PEMC admittance can be observed. In Fig. 5(a), in an isotropic plasma, a density plot of number density $(n)$ vs. PEMC admittance can be used to see the variation of the RCS or scattered electromagnetic field intensity for varied plasma densities and PEMC BCs. Elevated values of $n$ indicate an increase in collisions and intensified plasma interactions of VEMW, which affect wave propagation and wave attenuation; these factors, in turn, influence scattering characteristics. Admittance varies, transitioning from PMC to PEC at extreme values; however, for intermediate values, it remains as PEMC. This property regulates the reflection of VEMW at the PEMC surface. High $n$ and low PEMC admittance show that plasma characteristics like absorption and dispersion primarily influence scattering. RCS typically diminishes as a result of wave attenuation and interference. Low $n$ and high PEMC admittance specify enhanced reflective behaviour and this results in elevated RCS or pronounced backscattering. In intermediate region, the figure exhibits interference region where both plasma and BCs of PEMC surface nonlinearly influence the optical scattering.

In Fig. 5(b), the scattered field distribution under PEMC admittance and collision frequency $(v)$ can be seen. This influence affects plasma permittivity, leading to increased absorption as well as attenuation of LG VEMW. To get the best electromagnetic response, this density plot

is useful for tailoring plasma-material interactions. In summary, Table 1 presents the characteristics of the scattered field for a PEMC scatterer interacting with LG VEMW in an isotropic plasma, considering various values of collision frequency and PEMC admittance.

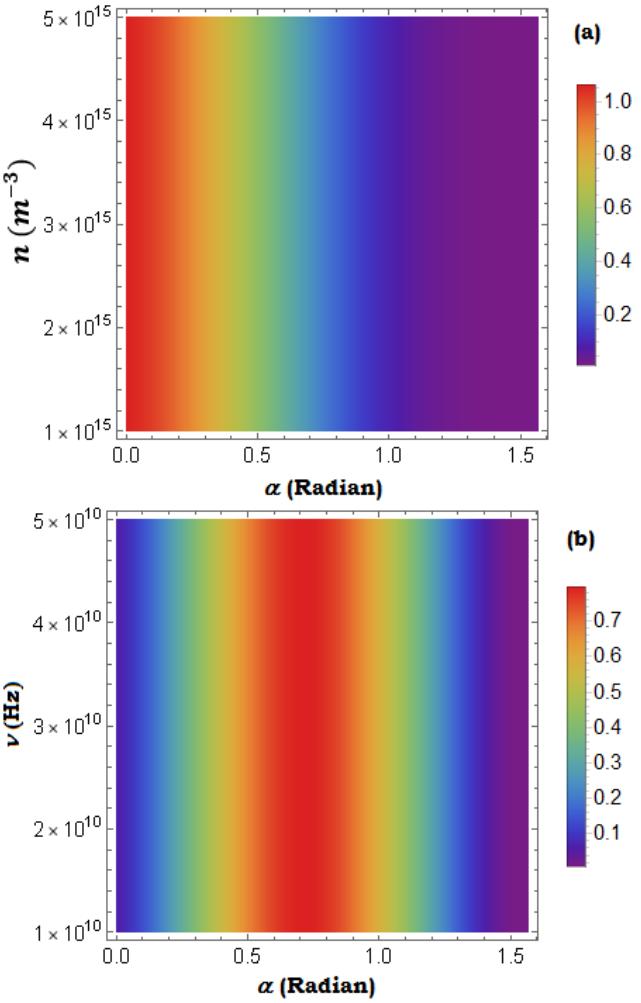


*Fig. 5. Density plot under number density $(n)$ and effective collision frequency $(\nu)$ with PEMC admittance (a) co-polarized scattered field component and (b) cross-polarized scattered field component (colour online)*

*Table 1. Scattered field distribution for various collision frequency and PEMC admittance*

| Collision frequency $(\nu)$ | PEMC admittance $(M)$ | RCS | Electromagnetic Characteristics |
|---|---|---|---|
| Low | Low | Increases | Strong wave reflection |
| High | Low | Decreases | More wave absorption |
| Low | High | RCS pattern varies | Dependence on VEMW polarization |
| High | High | Significant reduction | Maximum attenuation and minimal reflection |

## 4. Conclusions

The numerical results offered in this research yield significant insights, allowing for several conclusions to be outlined as follows:

- RCS of LG VEMW with configuration beam parameters, i.e., $p = 0\ \&\ l = 1$ considering a metamaterial PEMC sphere in the presence of an isotropic plasma, has been analyzed.
- The RCS can be regulated and optimized by selecting suitable isotropic plasma parameters, specifically plasma density $(n)$ and effective collision frequency $(\nu)$.
- The interactions of internal field modes due to OAM affect the scattering of VEMW, resulting in variations in the RCS response based on $n$ and $\nu$, which collectively influence scattering behaviour.
- Besides isotropic plasma parameters, PEMC admittance also tunes the scattering characteristics.
- The PEMC characteristic admittance parameter $(M)$ regulates the BCs between electromagnetic fields at the surface of PEMC. By adjusting the PEMC admittance, the interference phenomena between the incident and scattered electromagnetic fields can be controlled, which impacts field distribution.
- Adjusting the PEMC admittance allows for the manipulation of optical scattering characteristics, thereby optimizing the electromagnetic comeback for potential applications such as cloaking, and beam shaping, etc.
- The results indicate that the plasma medium can be used to adjust how the scattered field distributes, like the RCS of the PEMC sphere.
- In conclusion, the analysis of the RCS of a PEMC sphere in an isotropic plasma contributes to our comprehension of wave–matter interactions in engineered environments, thereby facilitating advancements in wave propagation, metamaterials, plasma-based sensing systems, and advanced communication systems.

### Acknowledgments

The authors extend their appreciation to Prince Sattam bin Abdulaziz University for funding this research work through the project number (PSAU/2020/01/17206).

## References

[1] L. Allen, M. W. Beijersbergen, R. Spreeuw, J. Woerdman, Physical Review A **45**, 8185 (1992).
[2] N. Biton, J. Kupferman, S. Arnon, Scientific Reports **11**, 1 (2021).
[3] C. L. Arnold, S. Akturk, A. Mysyrowicz, V. Jukna, A. Couairon, T. Itina, R. Stoian, C. Xie, J. Dudley, F. Courvoisier, Journal of Physics B: Atomic, Molecular

and Optical Physics **48**, 094006 (2015).
[4] M. Asif, M. Arfan, N. Khaleel, S. Althubiti, A. Althobaiti, Optical and Quantum Electronics **56**, 1474 (2024).
[5] V. V. Kotlyar, A. A. Kovalev, A. P. Porfirev, Vortex laser beams, CRC Press, 2018.
[6] G. Gouesbet, G. Gréhan, Generalized lorenz-mie theories, Springer, 2011.
[7] M. Cheng, W. Jiang, L. Guo, J. Li, A. Forbes, Light: Science & Applications **14**, 4 (2025).
[8] C. Liu, Journal of Physics: Conference Series, IOP Publishing **1549**, 3 032012 (2020).
[9] M. Arfan, M. Asif, S. Althobaiti, A. Althobaiti, Optical and Quantum Electronics **56**, 1610 (2024).
[10] F. Capolino, Theory and Phenomena of Metamaterials, CRC Press, 2017.
[11] F. Capolino, Applications of Metamaterials, CRC Press, 2017.
[12] A. L. Borja, Metamaterials: Devices and Applications, BoD–Books on Demand, 2017.
[13] M. Arfan, A. Ghaffar, M. A. S. Alkanhal, Y. Khan, A. H. Alqahtani, S. Ur Rehman, Arabian Journal for Science and Engineering **48**, 6 8001 (2022).
[14] A. Sihvola, I. V. Lindell, Theory and Phenomena of Metamaterials, CRC Press, pp. 26-21-26-27, 2017.
[15] I. V. Lindell, A. H. Sihvola, Journal of Electromagnetic Waves and Applications **19**, 861 (2005).
[16] A. Sihvola, I. V. Lindell, 2006 First European Conference on Antennas and Propagation, IEEE, pp. 1-4 (2006).
[17] M. Asif, M. Arfan, S. Althobaiti, A. Althobaiti, Y. Zhang, R. Li, H. Tang, Optical and Quantum Electronics **56**, 1242 (2024).
[18] Q. Chen, H. Qin, J. Liu, Scientific Reports **7**, 1 (2017).
[19] S. Khan, Results in Physics **7**, 4065 (2017).
[20] J. Fan, E. Parra, K. Kim, I. Alexeev, H. Milchberg, J. Cooley, T. Antonsen, Physical Review E **65**, 056408 (2002).
[21] Z. Lin, X. Chen, W. Qiu, J. Pu, Applied Sciences **8**, 665 (2018).
[22] D. Nobahar, S. Khorram, J. D. Rodrigues, Scientific Reports **11**, 16048 (2021).
[23] L. Xu, N. Yuan, IEEE Antennas and Wireless Propagation Letters **5**, 335 (2006).
[24] M. Hussan, A. Ghaffar, M. A. Alkanhal, M. Naz, S. Ur Rehman, Y. Khan, Physics of Plasmas **24**, 063303 (2017).
[25] A. Ghaffar, M. Yaqoob, M. A. Alkanhal, M. Sharif, Q. Naqvi, AEU-International Journal of Electronics and Communications **68**, 767 (2014).
[26] M. Vaheb, B. Ghalamkari, M. Naser-Moghadasi, IEEE Access **12**, 1-10 (2024).
[27] A. Ghaffar, M. Hussan, A. Illahi, M. A. Alkanhal, S. Ur Rehman, M. Naz, Waves in Random and Complex Media **28**, 35 (2018).
[28] M. Asghar, M. Qureshi, M. Akhtar, M. Fiaz, M. Ashraf, Journal of Modern Optics **64**, 101 (2017).
[29] N. Montaseri, A. Abdolali, M. Soleimani, V. Nayyeri, International Journal of RF and Microwave Computer-Aided Engineering **23**, 225 (2013).
[30] P. Acharya, A. M. Guzmán, Proc. SPIE **8011**, 451 (2011).
[31] C. Zhang, D. Chen, X. Jiang, Scientific Reports **7**, 154121 (2017).
[32] X. Bu, X. Liang, Z. Zhang, L. Chen, H. Tang, Z. Zeng, 2018 Progress in Electromagnetics Research Symposium (PIERS-Toyama), 801 (2018).
[33] L. Guo, Q. Huang, M. Cheng, J. Li, S. Liu, 2018 IEEE International Symposium on Antennas and Propagation & USNC/URSI National Radio Science Meeting, 2293 (2018).
[34] Z. Wu, T. Qu, J. Wu, Z. Wu, L. Yang, X. Li, IEEE Antennas and Wireless Propagation Letters **19**, 1365 (2020).
[35] M. Arfan, A. Ghaffar, M.A. Alkanhal, M. Naz, A. H. Alqahtani, Y. Khan, Optik **253**, 168562 (2022).
[36] M. Arfan, N. Khaleel, M. Asif, Iranian Journal of Science **47**, 1 (2023).
[37] J. A. Stratton, Electromagnetic theory, mcgrow-hill book company, Inc., New York, and London 1941.
[38] C. F. Bohren, D. R. Huffman, Absorption and scattering of light by small particles, John Wiley & Sons, 2008.
[39] R. Ruppin, Journal of Electromagnetic Waves and Applications **20**, 1569 (2006).

*Corresponding author: f.kasim@psau.edu.sa